Proton impurity in the neutron matter: A nuclear polaron problem

Marek Kutschera
H. Niewodniczański Institute of Nuclear Physics, ul. Radzikowskiego 152, 31-342 Kraków, Poland

Włodzimierz Wójcik
Institute of Physics, Technical University, ul. Podchorążych 1, 30-084 Kraków, Poland

(Received 1 October 1992)

We study interactions of a proton impurity with density oscillations of the neutron matter in a Debye approximation. The proton-phonon coupling is of the deformation-potential type at long wavelengths. It is weak at low density and increases with the neutron matter density. We calculate the proton's effective mass perturbatively for a weak coupling, and use a canonical transformation technique for stronger couplings. The proton's effective mass grows significantly with density, and at higher densities the proton impurity can be localized. This behavior is similar to that of the polaron in solids. We obtain properties of the localized proton in the strong-coupling regime from variational calculations, treating the neutron matter in the Thomas-Fermi approximation.

PACS number(s): 21.65.+f

I. INTRODUCTION

The number of protons present in the liquid core of neutron stars is of the order of a few percent [1] as compared with the number of neutrons. The proton admixture, which is required for the beta stability of the system, is found to decrease with density [1]. It eventually vanishes at some density n_v. Model calculations give n_v in the range $5n_0-10n_0$ [1]. Hence protons can be regarded as impurities in the neutron matter at densities close to n_v. Particularly important is the proton effective mass since it plays a crucial role for such phenomena in the neutron star matter as proton superfluidity [2] and/or possible spin instability [3].

The contributions to the proton's effective mass are generally of two types: The first one is due to two-body nuclear interactions while the other one is due to the coupling to excitations of the neutron matter. We shall denote corresponding values of the proton's effective mass m_* and $m_{\rm eff}$, respectively. At finite proton concentrations the latter contributions are expected to be small [4] and $m_* \approx m_{\rm eff}$. However, for a proton impurity, when the relevant energy scale is its vanishing kinetic energy, any phonon contribution can affect the effective mass profoundly, giving $m_{\rm eff}$ much higher than m_*.

In this paper we study the coupling of proton impurities in dense neutron matter to small density oscillations. This coupling can be quite strong as a result of the behavior of the proton chemical potential in the neutron matter. Various parametrization show that the proton chemical potential has a minimum close to the saturation density n_0. At higher densities the proton chemical potential increases and becomes positive at high densities (Fig. 1). This suggests that a uniform density neutron matter surrounding a proton might not be the lowest-energy state. Let us consider a neutron matter of density higher than the one corresponding to the minimum in Fig. 1, and imagine a small density fluctuation, such that the density around the proton is slightly reduced. For the long-wavelength fluctuation the proton energy is thus also reduced, as the proton moves now in an attractive potential well. This observation indicates that a single proton tends to disturb a uniform neutron matter, i.e., there appears a coupling of the proton to the (long-wavelength) neutron matter density oscillations. The coupling has a deformation-potential form.

The aim of this paper is to calculate the proton effective mass $m_{\rm eff}$ due to the proton-phonon coupling. The "nuclear" effective mass m_* derived from nuclear matter calculations will be used as a "bare" mass in our calculations. We treat phonons in the neutron matter in a Debye approximation. We use a perturbation theory

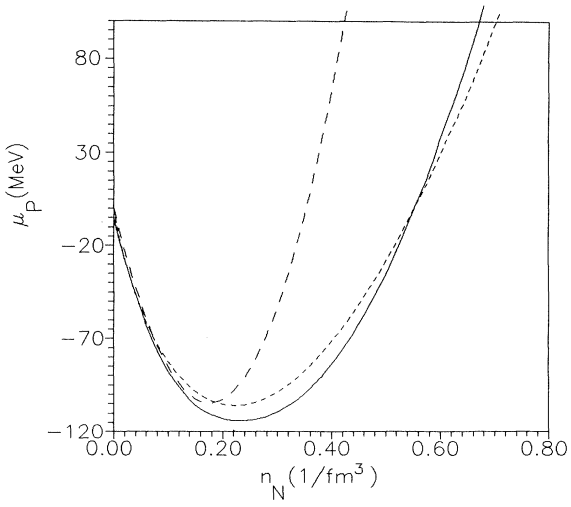

FIG. 1. The proton chemical potential in the neutron matter. The solid line is for the Friedman-Pandharipande-Ravenhall model (given in the Appendix) and dashed lines are for two Skyrme force parametrization of Ref. [8].

and a canonical transformation technique to calculate the proton effective mass for low and intermediate values of the coupling, respectively. The proton effective mass is found to increase with the neutron density. At higher densities, where the coupling becomes strong, one can expect a behavior similar to that of the polaron, which becomes localized in the strong coupling limit. We consider the case of strong-coupling variational Thomas-Fermi calculations which show localization of a single proton in neutron matter above a critical density n_c which, however, depends strongly on m_*.

As we mentioned, the phenomenon we consider has a well-known analog in solid-state physics. In some crystals the electron-phonon interactions influence the effective mass of electrons significantly [5,6]. The system consisting of the electron and the virtual phonon cloud is called a polaron. Above a critical coupling the polaron becomes localized and the corresponding effective mass is very large [5,6].

In Sec. II we derive the interaction Hamiltonian which couples the proton to the neutron matter density oscillations. In Sec. III we calculate the proton effective mass in the first-order perturbation theory, for the weak coupling, and by a canonical transformation technique for stronger couplings. In Sec. IV a possibility of localization in the case of strong coupling is considered. The results are discussed in Sec. V.

II. COUPLING OF A PROTON IMPURITY TO PHONONS IN NEUTRON MATTER

Let us consider a single proton in a uniform neutron matter of density n_N. If the momentum $\mathbf{k}$ of the proton is low, the energy of the proton is

$$E_P(\mathbf{k}) \cong \frac{\mathbf{k}^2}{2m_*} + v_{\text{eff}} , \tag{1}$$

where the effective potential is equal to the proton chemical potential in a neutron matter,

$$v_{\text{eff}} = \mu_P(n_N) . \tag{2}$$

The chemical potential $\mu_P(n_N)$ is the energy of a zero-momentum proton. Here m_* is the effective mass of the proton due to nuclear interactions with neutrons and it does not include any phonon contribution. The effective potential can, in principle, depend on the proton momentum; however, this is higher order and can be neglected for small values of $\mathbf{k}$. We can thus write the Hamiltonian of the slow proton in the form

$$H_P^{(0)} = -\frac{\nabla^2}{2m_*} + \mu_P(n_N) . \tag{3}$$

Assume now that the neutron matter is slightly inhomogeneous, with the neutron density

$$n(\mathbf{r},t) = n_N + \delta n(\mathbf{r},t) , \tag{4}$$

where δn is a small perturbation. If the density $n(\mathbf{r},t)$ varies sufficiently slowly, i.e., the wavelength of the perturbation is sufficiently long and the frequency is low, the proton energy is still given by Eq. (1). Hence the Hamiltonian of the single proton in the neutron matter with small long-wavelength oscillations is

$$H_P = -\frac{\nabla^2}{2m_*} + \mu_P(n_N) + \frac{\partial \mu_P}{\partial n_N}\delta n(\mathbf{r},t) = H_P^{(0)} + H_{\text{int}} . \tag{5}$$

The last term describes the coupling of the proton to the small oscillations of the neutron matter density.

For long-wavelength oscillations the neutron matter can be treated as a continuous medium, and standard methods of describing phonons in the medium [6] can be used. The density oscillations can be expressed by the displacement $\mathbf{u}(\mathbf{r},t)$ of the neutron matter from its equilibrium position

$$\delta n(\mathbf{r},t) = n(\mathbf{r},t) - n_N = -n_N \nabla \mathbf{u} . \tag{6}$$

We can expand the displacement field $\mathbf{u}$ in the normal modes (phonons):

$$\mathbf{u}(\mathbf{r},t) = \frac{1}{\sqrt{V}} \sum_{\mathbf{k}} \frac{1}{\sqrt{2En_N\omega(\mathbf{k})}} \times e(\mathbf{k})(a_{\mathbf{k}} e^{i\mathbf{k}\cdot\mathbf{r}} + a_{\mathbf{k}}^{+} e^{-i\mathbf{k}\cdot\mathbf{r}}) , \tag{7}$$

where $\mathbf{e}(\mathbf{k})$ is the unit polarization vector, E is the energy per neutron (including the rest mass) in neutron matter of density n_N, and $\omega(\mathbf{k})$ is the energy of the phonon of momentum $\mathbf{k}$. For longitudinal acoustical phonons $\mathbf{e}(\mathbf{k})$ is parallel to $\mathbf{k}$ and $\omega(\mathbf{k}) = c_s|\mathbf{k}|$, where c_s is the velocity of acoustical waves in the neutron matter.

Quantization of the phonon field can be carried out in a standard way replacing the Fourier component $a_{\mathbf{k}}(t) = a_{\mathbf{k}}\exp[-i\omega(\mathbf{k})t]$ by the phonon annihilation operator. The interaction Hamiltonian becomes

$$H_{\text{int}} = \frac{1}{\sqrt{V}} \sum_{q} [B(\mathbf{q}) a_{\mathbf{q}} \exp(i\mathbf{q}\cdot\mathbf{r}) + B(\mathbf{q})^* a_{\mathbf{q}}^{\dagger} \exp(-i\mathbf{q}\cdot\mathbf{r})] , \tag{8}$$

where

$$B(\mathbf{q}) = -i\frac{\partial \mu_P}{\partial n_N}(n_N) n_N \left[\frac{|\mathbf{q}|}{2Ec_s n_N}\right]^{1/2} . \tag{9}$$

Expanding also the proton wave function in the plane basis,

$$\Psi_P(\mathbf{r}) = \frac{1}{\sqrt{V}} \sum_{\mathbf{k}} c_{\mathbf{k}} e^{i\mathbf{k}\cdot\mathbf{r}} , \tag{10}$$

we can write the interaction Hamiltonian in terms of phonon and proton annihilation and creation operators

$$\hat{H}_{\text{int}} = \int d^3r\, \Psi_P^*(\mathbf{r}) \frac{\partial \mu_P}{\partial n_N}\delta n(\mathbf{r},t)\Psi_P(\mathbf{r}) = \frac{1}{\sqrt{V}} \sum_{\mathbf{k},\mathbf{q}} B(\mathbf{q}) c_{\mathbf{k}+\mathbf{q}}^{\dagger} c_{\mathbf{k}} (a_{\mathbf{q}} - a_{-\mathbf{q}}^{\dagger}) . \tag{11}$$

The proton-phonon coupling (11) has the form of the deformation-potential coupling in solids [6], with the deformation-potential constant

$$\sigma=\frac{\partial\mu_P}{\partial n_N}(n_N)n_N \ . \tag{12}$$

This quantity measures the strength of the proton-phonon coupling. Since it is a product of the derivative of the proton chemical potential, with respect to the neutron density, and the neutron density itself, it is small at low densities and near the minimum in Fig. 1. For higher densities σ increases linearly (Fig. 2). In the following we shall consider only the high density range which extends to the right of the minimum in Fig. 1. The proton-phonon coupling is thus weak near the minimum and becomes strong at high density.

III. WEAK AND INTERMEDIATE PROTON-PHONON COUPLING

The interaction Hamiltonian (11) can be treated as a small perturbation of the energy of a proton in a uniform density neutron matter $H_P^{(0)}$, Eq. (3), in case of low values of $B(\mathbf{q})$. We now consider this case.

A. Perturbative calculations

The lowest-order perturbation correction is obtained for single-phonon intermediate states [6]. The first-order wave function, in the Fock representation, is

$$\Psi_{\mathbf{k},0}=|\mathbf{k},0_\mathbf{q}\rangle+(-1)\sum_{\mathbf{k}_1,\mathbf{q}}\frac{|\mathbf{k}_1,1_\mathbf{q}\rangle\langle\mathbf{k}_1,1_\mathbf{q}|\hat{H}_{\rm int}|\mathbf{k},0\rangle}{D(\mathbf{k},\mathbf{q})} \ , \tag{13}$$

where the matrix element of the interaction Hamiltonian is

$$\langle\mathbf{k}_1,1_\mathbf{q}|\hat{H}_{\rm int}|\mathbf{k},0\rangle=\frac{1}{\sqrt{V}}B(\mathbf{q})\delta_{\mathbf{k}_1,\mathbf{k}-\mathbf{q}} \tag{14}$$

and

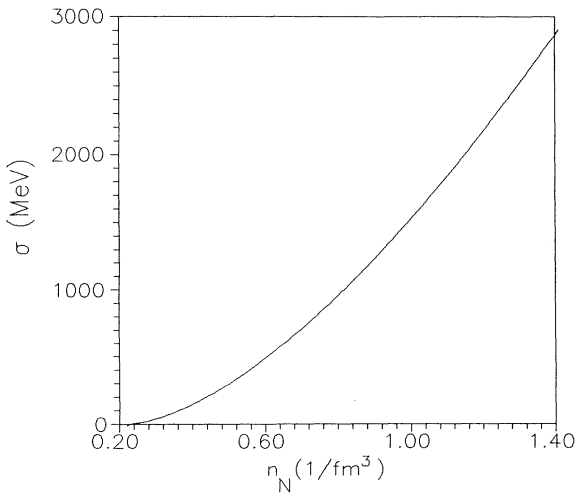

FIG. 2. The deformation-potential coupling strength as a function of neutron matter density for the Friedman-Pandharipande-Ravenhall model.

$$D(\mathbf{k},\mathbf{q})=E_P(\mathbf{k}-\mathbf{q})+\omega(\mathbf{q})-E_P(\mathbf{k}) \ . \tag{15}$$

We use here a standard notation [6], in which the single-phonon states $|\mathbf{k},1_\mathbf{q}\rangle$ are defined by the proton momentum $\mathbf{k}$ and the phonon momentum $\mathbf{q}$. The wave function (13) is thus

$$\Psi_{\mathbf{k},0}=|\mathbf{k},0_\mathbf{q}\rangle+\frac{1}{\sqrt{V}}\sum_\mathbf{q}\frac{|\mathbf{k}-\mathbf{q},1_\mathbf{q}\rangle}{D(\mathbf{k},\mathbf{q})}B(\mathbf{q}) \ . \tag{16}$$

Using the wave function (16) we can calculate the energy of the proton impurity up to the second order in the interaction, which is

$$E_P^{(2)}(\mathbf{k})=\frac{\mathbf{k}^2}{2m_*}+v_{\rm eff}-\sum_\mathbf{q}\frac{|\langle\mathbf{k}-\mathbf{q},1_\mathbf{q}|\hat{H}_{\rm int}|\mathbf{k},0\rangle|^2}{D(\mathbf{k},\mathbf{q})} \ . \tag{17}$$

Evaluating the last contribution in the expression (17) we can find the proton effective mass, as well as the change of the proton energy due to the coupling to phonons. For small values of $\mathbf{k}$ one can expand

$$\frac{1}{D(\mathbf{k},\mathbf{q})}\cong\frac{2m_*}{q(q+Q)}\left[1+\frac{2k\nu}{q+Q}+\frac{4k^2\nu^2}{(q+Q)^2}\right] \ . \tag{18}$$

Here $k=|\mathbf{k}|$, $q=|\mathbf{q}|$, $Q=2m_*c_s$, and ν is the cosine of the angle between $\mathbf{k}$ and $\mathbf{q}$.

The sum over the phonon momenta $\mathbf{q}$ can be replaced for the single-phonon states, in a Debye approximation, by the integral

$$\frac{1}{V}\sum_\mathbf{q}\rightarrow\frac{1}{(2\pi)^3}\int_0^{q_{\rm max}}d^3q \ , \tag{19}$$

where $q_{\rm max}$ is the Debye cutoff momentum. It has a physical origin: In the neutron matter the wavelength of phonons is limited by the interparticle distance. The results presented below correspond to putting the Debye phonon momentum equal to the Fermi momentum of the neutron matter, $q_{\rm max}=k_N$.

From Eqs. (17) and (18) we find

$$\frac{1}{2m_{\rm eff}}=\frac{1}{2m_*}-\left[\frac{\partial\mu_P}{\partial n}(n_N)\right]^2\frac{2m_*n_N}{3\pi^2Ec_s}I_2 \ , \tag{20}$$

where I_2 is

$$I_2=\ln\left[1+\frac{q_{\rm max}}{Q}\right]-\tfrac{1}{2}+\frac{(Q/q_{\rm max})^2-2}{2(Q/q_{\rm max}+1)^2} \ . \tag{21}$$

The correction to the proton energy is

$$\Delta E_P=-\left[\frac{\partial\mu_P}{\partial n}(n_N)\right]^2\frac{m_*n_N}{Ec_s}\frac{q_{\rm max}^2}{2\pi^2}I_1 \ , \tag{22}$$

where I_1 reads

$$I_1=\tfrac{1}{2}-\frac{Q}{q_{\rm max}}+\left[\frac{Q}{q_{\rm max}}\right]^2\ln\left[1+\frac{q_{\rm max}}{Q}\right] \ . \tag{23}$$

An important quantity, which can be used to control the breakdown of the first-order approximation, is the number of virtual phonons. It is given by the formula

$$\langle \nu_{\mathbf{k},0} \rangle = \sum_{\mathbf{q}} \frac{1}{D(\mathbf{k},\mathbf{q})^2} |B(\mathbf{q})|^2 , \tag{24}$$

which, after evaluating the sum, becomes

$$\langle \nu_{\mathbf{k},0} \rangle = \left[\frac{\partial \mu_P}{\partial \mu_N}(n_N) \right]^2 \frac{m_*^2 n_N}{E c_s} \frac{1}{\pi^2} \left[\ln \left[1 + \frac{q_{\max}}{Q} \right] - \frac{1}{Q/q_{\max}+1} \right] . \tag{25}$$

B. Canonical transformation method

As a signal of breakdown of perturbative calculations one can use the number of virtual phonons (25). When it exceeds unity the first-order approximation becomes invalid. This already happens at rather low density. For higher densities, i.e., for higher coupling, we shall use the canonical transformation method of Lee, Low, and Pines [7]. It can be summarized as follows.

One starts with the interaction Hamiltonian H_{int}, Eq. (8), and the "free" proton Hamiltonian $H_P^{(0)}$, Eq. (3). The full Hamiltonian of the proton-phonon system reads

$$H = H_P^{(0)} + H_{\text{int}} + H_{\text{ph}} , \tag{26}$$

where the phonon Hamiltonian H_{ph} is

$$H_{\text{ph}} = \sum_{\mathbf{q}} \omega(\mathbf{q}) a_{\mathbf{q}}^{\dagger} a_{\mathbf{q}} . \tag{27}$$

The Hamiltonian (27) commutes with the momentum operator

$$\hat{\mathbf{P}} = \sum_{\mathbf{q}} \mathbf{q} a_{\mathbf{q}}^{\dagger} a_{\mathbf{q}} + \mathbf{P} , \tag{28}$$

where $\mathbf{p}$ is the proton momentum. One can thus transform to a representation in which $\hat{\mathbf{P}}$ is diagonal and in which the Hamiltonian does not contain the proton coordinates. This is obtained [7] by applying the canonical transformation

$$S = \exp \left[i \left[\mathbf{P} - \sum_{\mathbf{q}} \mathbf{q} a_{\mathbf{q}}^{\dagger} a_{\mathbf{q}} \right] \cdot \mathbf{r} \right] . \tag{29}$$

The transformed Hamiltonian reads

$$H = \frac{1}{2m_*} \left[\mathbf{P} - \sum_{\mathbf{q}} \mathbf{q} a_{\mathbf{q}}^{\dagger} a_{\mathbf{q}} \right]^2 + \sum_{\mathbf{q}} \omega(\mathbf{q}) a_{\mathbf{q}}^{\dagger} a_{\mathbf{q}} + \sum_{\mathbf{q}} F(\mathbf{q})(a_{\mathbf{q}} - a_{-\mathbf{q}}^{\dagger}) , \tag{30}$$

where

$$F(\mathbf{q}) = \frac{1}{\sqrt{V}} B(\mathbf{q}) . \tag{31}$$

The ground state of the system for a given momentum $\mathbf{P}$ is calculated variationally [7], replacing the displacement operator

$$Q_{\mathbf{q}} = q_{\mathbf{q}} + a_{\mathbf{q}}^{\dagger} \tag{32}$$

by its expectation value

$$\langle Q_{\mathbf{q}} \rangle = f_{\mathbf{q}} + f_{\mathbf{q}}^* . \tag{33}$$

This is achieved by a new canonical transformation

$$U = \exp \left[\sum_{\mathbf{q}} (f_{\mathbf{q}} a_{\mathbf{q}}^{\dagger} - f_{\mathbf{q}}^* a_{\mathbf{q}}) \right] , \tag{34}$$

where $f_{\mathbf{q}}$ will be chosen to minimize the energy. This transformation shifts the phonon creation and annihilation operators:

$$U^{-1} a_{\mathbf{q}}^{\dagger} U = a_{\mathbf{q}}^{\dagger} + f_{\mathbf{q}}^{\dagger} , \quad U^{-1} a_{\mathbf{q}} U = a_{\mathbf{q}} + f_{\mathbf{q}} . \tag{35}$$

The phonon-vacuum expectation value of the transformed Hamiltonian is

$$E = \frac{\mathbf{P}^2}{2m_*} + \sum_{\mathbf{q}} F(\mathbf{q})(f_{\mathbf{q}} - f_{\mathbf{q}}^*) + \frac{1}{2m_*} \left[\sum_{\mathbf{q}} \mathbf{q} |f_{\mathbf{q}}|^2 \right]^2 + \sum_{\mathbf{q}} |f_{\mathbf{q}}|^2 \left[\omega(\mathbf{q}) - \frac{1}{m_*} \mathbf{P} \cdot \mathbf{q} + \frac{1}{2m_*} \mathbf{q}^2 \right] . \tag{36}$$

Minimizing E, Eq. (36), we find the following equation for $f_{\mathbf{q}}$:

$$f_{\mathbf{q}} \left[\omega(\mathbf{q}) - \frac{1}{m_*} \mathbf{P} \cdot \mathbf{q} + \frac{1}{2m_*} \mathbf{q}^2 + \frac{1}{m_*} \sum_{\mathbf{s}} |f_{\mathbf{s}}|^2 \mathbf{s} \cdot \mathbf{q} \right] = F(\mathbf{q}) . \tag{37}$$

In order to solve this equation one can write [7]

$$\sum_{\mathbf{q}} \mathbf{q} |f_{\mathbf{q}}|^2 = \zeta \mathbf{P} \tag{38}$$

since the only available vector is $\mathbf{P}$. Putting $f_{\mathbf{q}}$, Eq. (37), into Eq. (38) and linearizing the left-hand side for small values of $|\mathbf{P}|$, one can solve for ζ:

$$\zeta = \frac{2Am_*}{1+2Am_*} , \tag{39}$$

where

$$A = \left[\frac{\partial \mu_P}{\partial \mu_N}(n_N) \right]^2 \frac{2m_* n_N}{3Ec_s \pi^2} I_2 . \tag{40}$$

Finally, the following expression for the proton effective mass is obtained:

$$\frac{1}{2m_{\text{eff}}} = \frac{1}{2m_*}(1-\zeta^2) - A(1-\zeta)^2 . \tag{41}$$

The change of the proton energy is given by the same formula as in perturbative calculations above, Eq. (22).

To evaluate numerically the above formulas we must specify a number of quantities. The most important quantity in our calculations is the proton chemical potential in the neutron matter. To obtain it we use the Ravenhall's parametrization, as given in Ref. [8], of the nuclear matter calculations of Friedman and Pandharipande [9]. This multiparameter fit is given in the Appendix. The results of Friedman and Pandharipande [9] are thought to be one of the most reliable neutron matter calculations. The proton chemical potential for the Friedman-Pandharipande-Ravenhall (FPR) nuclear interactions is displayed in Fig. 1. For comparison, we also

show curves corresponding to different Skyrme force parametrization from Ref. [8].

The strength of the proton-phonon coupling σ, Eq. (12), is derived from the proton chemical potential. One can notice in Fig. 2 that this coupling strength is a linear function of the neutron density at high densities.

The second quantity we must specify is the proton effective mass m_* in neutron matter due to nuclear interactions. Sjöberg [4] calculated m_* in strongly asymmetric nuclear matter, containing a small proton fraction, in the framework of the Landau Fermi-liquid theory. He has found m_* to be about a half of the bare mass and slightly decreasing with density. We use here for m_* the values obtained in the Appendix for the FPR parametrization (dashed curve 1 in Fig. 3). These are somewhat lower than the Sjöberg's mass. For comparison we also present results corresponding to the bare proton mass $m_*=939$ MeV. The effective mass m_* serves as a bare mass in our calculations.

The last important quantity is the sound velocity c_s in the neutron matter. In order to calculate its value one should discuss the nature of density waves in the neutron matter. This is beyond the scope of the present paper. Let us only mention that at zero temperature there exists a zero sound in degenerate Fermi systems. The normal sound, however, cannot propagate. For neutron matter the zero sound velocity was calculated by Haensel [10], who has found the values $c_s=0.6-0.7$. In real physical systems where the neutron matter is present, i.e., in neutron stars, the temperature is low as compared to the Fermi energy, but it may be still high enough, that normal sound can also exist [11]. In our calculations we adopt the values obtained by Haensel [10].

The main results are presented in Fig. 3 where we show the proton effective mass m_{eff}, Eq. (41), as a function of the neutron matter density for two different choices of the bare mass m_*. The curves labeled 1 and 2 correspond to $m_*=939$ MeV and the values obtained from the FPR formula in the Appendix, respectively. The variational results, Eq. (41), are shown as solid lines. One should notice that the behavior of the proton effective mass is similar in both cases: The effective mass starts to increase significantly at the density about $3n_0$ and becomes twice the bare mass at about $4n_0$. For comparison we also show perturbative results, Eq. (20) (long-dashed lines). The effective mass in this case has a singularity, however, it occurs outside the range of validity of the first-order perturbation theory.

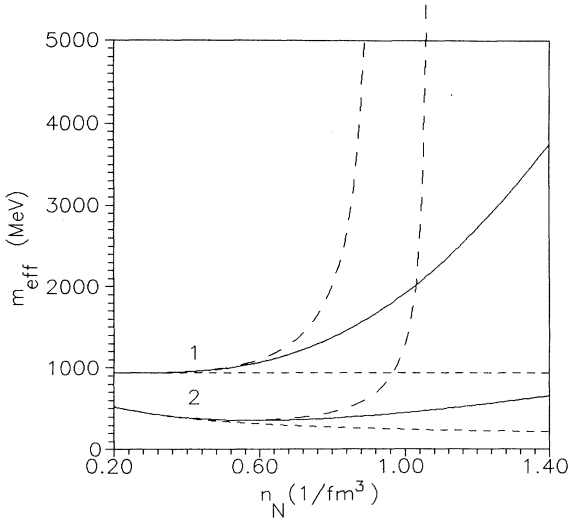

FIG. 3. The proton effective mass as a function of neutron density. Solid lines are the canonical transformation technique results and long-dashed lines are the perturbative results. Short-dashed lines represent the effective mass m_*. The labels 1 and 2 correspond to $m_*=939$ MeV and to the FPR m_*, respectively.

The single-phonon approximation is justified as long as the number of phonons is less than on [6]. In Fig. 4 we show the number of phonons as a function of neutron matter density for two different "bare" proton masses. It is higher for $m_*=939$ MeV (dashed line) than for the FPR proton mass m_*, which decreases with the density (solid line). The condition of validity is satisfied for densities below $5n_0$ (solid line) and $4n_0$ (dashed line), respectively.

Let us finally mention that by changing the values of the sound velocity c_s and the cutoff phonon momentum $q_{\max}$ one also changes the results shown in the Figs. 3 and 4. Higher values c_s move the singularity in the effective mass to higher densities, and the same happens for lower values of $q_{\max}$. The general behavior, however, is not very sensitive to such variations.

IV. STRONG PROTON-PHONON COUPLING: LOCALIZATION OF PROTON IMPURITIES?

It is instructive to express the wave function (16) in the coordinate representation in order to see that there is a tendency for localization. The wave function (16) can be written in the form

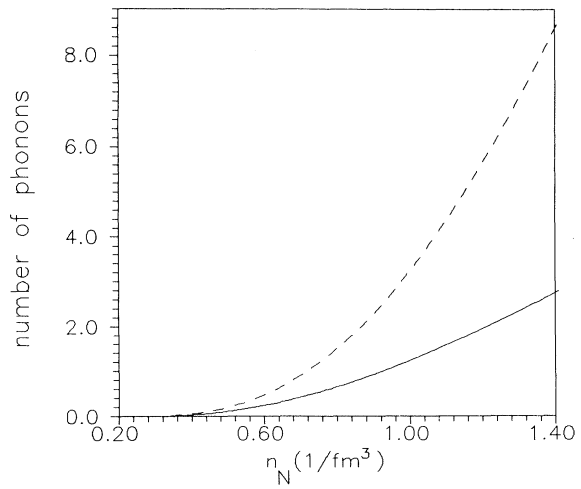

FIG. 4. The mean number of virtual phonons. Solid and dashed lines correspond to the FPR m_* and $m_*=939$ MeV, respectively.

$$\Psi(\mathbf{r})=\frac{1}{\sqrt{V}}e^{i\mathbf{k}\cdot\mathbf{r}}\left[1+\frac{1}{\sqrt{V}}\sum_{\mathbf{q}}\frac{e^{-i\mathbf{q}\cdot\mathbf{r}}B(\mathbf{q})}{D(\mathbf{k},\mathbf{q})}a_{\mathbf{q}}^{\dagger}\right]|0\rangle$$
$$=\frac{1}{\sqrt{V}}e^{i\mathbf{k}\cdot\mathbf{r}}\eta(\mathbf{r})|0\rangle\ , \tag{42}$$

where $|0\rangle$ is the phonon vacuum. The approximate form of the function $\eta(\mathbf{r})$ can be obtained using the variational method of the previous section. The operator $a_{\mathbf{q}}^{\dagger}$ can be replaced by $f_{\mathbf{q}}^{*}$. We approximate $f_{\mathbf{q}}^{*}$ assuming $\zeta=0$:

$$f_{\mathbf{q}}^{*}\approx\frac{1}{\sqrt{V}}\frac{B^{*}(\mathbf{q})}{D(\mathbf{k},\mathbf{q})}\ . \tag{43}$$

The function $\eta(\mathbf{r})$ now reads

$$\eta(\mathbf{r})=1+\frac{1}{V}\sum_{\mathbf{q}}\frac{e^{-i\mathbf{q}\cdot\mathbf{r}}|B(\mathbf{q})|^2}{D(\mathbf{k},\mathbf{q})^2}\ . \tag{44}$$

For a zero-momentum proton there is a spherical symmetry and one finds

$$\eta(r)=1+\left[\frac{\partial\mu_P}{\partial\mu_N}(n_N)\right]^2\frac{m_*^2 n_N}{Ec_s}\frac{1}{\pi^2}\frac{1}{r}\int_0^{q_{\max}}dq\frac{\sin(qr)}{(q+Q)^2}\ . \tag{45}$$

The last integral can be expressed by the integral sine and cosine functions.

We show the function $\eta(r)$ in Fig. 5 for a few values of the neutron density. One can see, that although the proton is not localized, the probability to find it near the origin is enhanced. The origin $r=0$ is chosen as a center of the neutron density displacement. Generally, with increased density the value of $\eta(0)$ increases. This process is accompanied by a displacement of the neutron matter which has a maximum slope at the origin. According to Eq. (6), the corresponding density fluctuation is also at its largest at the origin, i.e., the potential well has its bottom there. One thus finds that the interaction of the (zero-momentum) proton with the phonons results in a deformation of the neutron background which in turn attracts the proton.

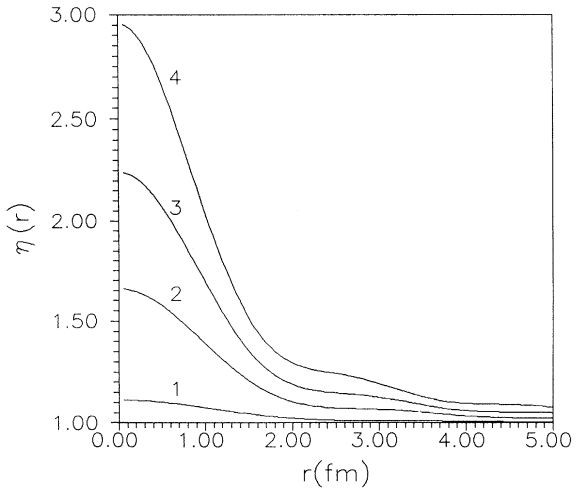

FIG. 5. The function $\eta(r)$, Eq. (45), for various densities. Curves 1–4 correspond respectively to neutron density 0.5, 0.8, 1, and 1.2 fm^{-3}.

One can easily imagine that with increased coupling the neutron density fluctuations become larger, and the potential well felt by the proton becomes deeper. We can ask a question if there exists a critical coupling above which the potential well becomes deep enough to bind the proton. The proton wave function would be localized in such a potential well.

To describe this state we shall treat the Hamiltonian (5) in a local-density approximation [12]. We must also take into account the neutron background since now the deformation is real. To see if the proton can be localized we compare energies of two phases: a normal phase and a phase with localized protons. The energy of the latter one is calculated variationally, treating the neutron background in the Thomas-Fermi approximation. In the spirit of the Wigner-Seitz approximation we divide the system into cells, each of them enclosing a single proton. For simplicity the cells are assumed to be spherical. The volume of the cell is $V=1/n_P$, where n_P is the proton density. In the following we consider limit $V\to\infty$.

The normal phase is of uniform neutron density n_N. In this phase protons are not localized and their wave functions are plane waves. The energy of the cell, which is a sum of proton and neutron energies, for small proton density n_P, is approximately

$$E_0\approx\mu_P(n_N)+V\epsilon(n_N)\ . \tag{46}$$

In the localized phase the protons are trapped into potential wells, corresponding to the nonuniform neutron density distribution. Let us consider a Wigner-Seitz cell with nonuniform neutron matter distribution $n(r)$ surrounding the proton whose wave function is Ψ_P. In the local density approximation the proton's effective potential varies locally with neutron matter density $n(r)$. We identify this effective potential with the local proton chemical potential $\mu_p(n)$. This results in a potential well $\mu_P(n(r))$ which affects the single proton wave function.

The energy of the Wigner-Seitz cell is

$$E_L=\int_V d^3r\,\Psi_P^{*}(r)\left[-\frac{\nabla^2}{2m_*}+\mu_P(n(r))\right]\Psi_P(r)$$
$$+\int_V d^3r\,\epsilon(n(r))+B_N\int_V d^3r[\nabla n(r)]^2\ . \tag{47}$$

The first term is the energy of the proton confined to an effective potential well $v_{\text{eff}}(r)=\mu_P(n(r))$. This is by construction an attractive potential well. At high densities the derivative of the proton chemical potential is positive and $n(r)$ is assumed to have a minimum at the center of the cell.

The two other terms in Eq. (47) describe the neutron background contributions to the energy. These represent the neutron Fermi sea energy and the curvature energy due to the gradient of the neutron distribution, respectively, in the Thomas-Fermi approximation. Here $\epsilon(n(r))$ is the local neutron matter energy per unit volume. The parameter B_N is the curvature coefficient for pure neutron matter.

In order to decide which is the ground-state

configuration we should compare the energies E_0, Eq. (46), and E_L, Eq. (47), assuming the same number of neutrons in the cell:

$$\int_V d^3r\, n(r) = V n_N \ . \tag{48}$$

This means that the neutron density variation $\delta n(r) = n(r) - n_N$ conserves the baryon number:

$$\int_V d^3r\, \delta n(r) = 0 \ . \tag{49}$$

Calculations presented here are variational. We assume a simple trial form of the proton wave function and the neutron density variation. For the proton wave function we use a Gaussian:

$$\Psi_P(r) = \left[\frac{2}{3}\pi R_P^2\right]^{-3/4} \exp\left[-\frac{3r^2}{4R_P^2}\right] \ . \tag{50}$$

Here R_P is the rms radius of the localized proton probability distribution. We treat this quantity as a variational parameter and minimize the energy difference $\Delta E = E_L - E_0$ with respect to R_P.

The neutron density variation $\delta n(r)$, satisfying Eq. (49), is also chosen to have a Gaussian shape:

$$\delta n(r) = \alpha \left[\frac{2}{3}\pi R_N^2\right]^{-3/2} \exp\left[-\frac{3r^2}{2R_N^2}\right] - \alpha \frac{1}{V} \ , \tag{51}$$

where R_N is the rms radius of the neutron distribution and α is the amplitude of the neutron density variation. The neutron density is

$$n(r) = n_N + \delta n(r) \ . \tag{52}$$

We assume R_N and α to be variational parameters; $\alpha > 0$ corresponds to the neutron density enhancement around the proton and $\alpha < 0$ corresponds to the reduction of the neutron density in the proton vicinity as compared with the uniform background. The neutron density $n(r)$, the proton's probability distribution, and the potential well $v_{\text{eff}}(r)$ are shown in Figs. 6 and 7 in a specific case.

Using the trial forms of the proton wave function and the neutron density variation the energy difference ΔE becomes

$$\begin{aligned}\Delta E = {} & \frac{9}{8m_*}\frac{1}{R_P^2} + \int_V d^3r\, \Psi_P^*(r)[\mu_P(n(r)) \\ & - \mu_P(n_N)]\Psi_P(r) \\ & + \int_V d^3r[\epsilon(n(r)) - \epsilon(n_N)] \\ & + B_N \alpha^2 \frac{9}{2}\left[\frac{4\pi}{3}\right]^{-3/2} \frac{1}{R_N^5} \ .\end{aligned} \tag{53}$$

The first term is the proton kinetic energy. The second term, which is attractive, originates from the interaction of the proton with the neutron background. The third term accounts for the local change of the neutron Fermi momentum. The last term is due to the gradient term in Eq. (47). This term plays a stabilizing role for small values of R_N.

We have evaluated the energy ΔE for the FPR model of nuclear interactions. The energy ΔE as a function of the proton localization radius displays a typical polaron behavior [6]: It is positive for both very large and very small values of R_P with a negative minimum occurring at intermediate R_P. The density, at which ΔE becomes negative, is the critical density for proton localization.

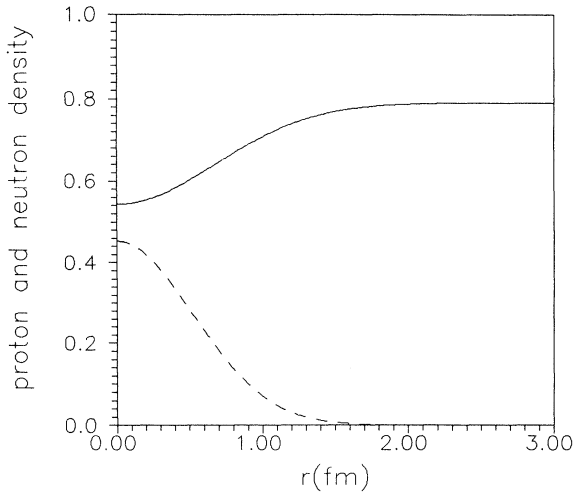

FIG. 6. The proton probability distribution (dashed line) and neutron density distribution (solid line) in the Wigner-Seitz cell. The neutron density is $n_N = 0.8\ \text{fm}^{-3}$.

In Fig. 8 we show the minimum energy difference ΔE_m obtained by minimizing ΔE for two choices of m_*. For $m_* = 939$ MeV (curves 1) the minimum occurs for $R_N \approx 1.3 R_P$ and $\alpha = -1.2$. The gradient term coefficient $B_N = 31.6\ \text{MeV fm}^5$ is used [12,13]. Also, results for $B_N = 0$ are shown. We only show negative values of ΔE, which indicate that the localized protons form the ground state of the system. The critical density is $n_c \approx 4 n_0$. For the FPR effective mass m_* (curves 2) the minimum occurs for $R_N \approx 1.3 R_P$ and $\alpha = -2$. The critical density is higher, $n_c \approx 9 n_0$. Corresponding effective

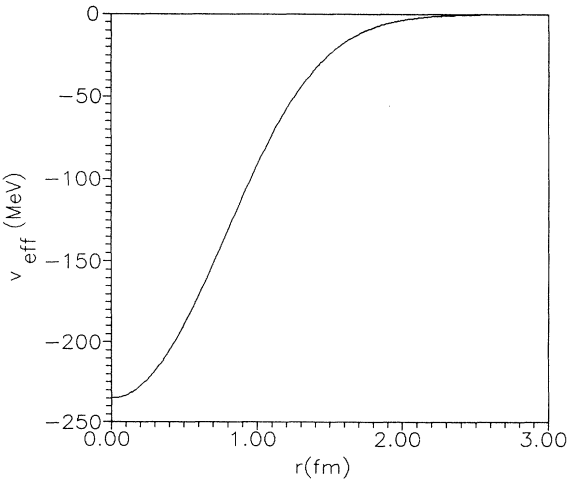

FIG. 7. The effective potential well in which the proton is localized for neutron density $n_N = 0.8\ \text{fm}^{-3}$.

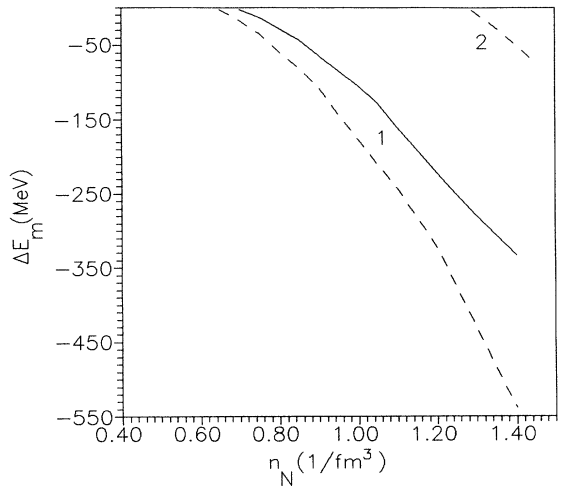

FIG. 8. Binding energy of localized proton. The labels 1 and 2 correspond to $m_*=939$ MeV and the FPR m_*, respectively. Solid line is for $B_N=31.6$ MeV fm^5 and dashed lines are for $B_N=0$.

mass is $m_*\approx 220$ MeV. The critical density n_c turns out to be quite sensitive to the value of the effective mass m_* used in the kinetic-energy term in Eq. (53).

V. CONCLUSIONS AND DISCUSSION OF THE RESULTS

We have shown, in simple model calculations, that the effective mass of a proton impurity in the neutron matter can be much higher than the "bare" mass as a result of a strong proton-phonon coupling. At high densities the proton impurity can eventually be localized. This behavior is in contrast to the Fermi-liquid case [4] when protons form a Fermi sphere. The reason is that while the phonon contribution to the proton energy can be small compared with the Fermi energy, it is always large when compared with (zero) kinetic energy of the impurity. One can expect that other excitations coupled to the proton impurity can further increase its effective mass.

The problem we consider here is similar to that of an electron interacting with phonons in solids, which is called the polaron. The mechanism of a self-trapping of a proton into the potential well produced by the deformed neutron background is analogous to that of localization of an electron strongly coupled to lattice vibrations (small polaron). In particular, the proton-phonon Hamiltonian (11) has precisely the form of the deformation potential introduced by Bardeen and Shockley [14] to describe electron-phonon interaction in covalent crystals. The polaron problem is thoroughly treated in textbooks [5,6]. The most interesting feature is the localization of the polaron above a critical value of the coupling constant: The electron is trapped into the potential well due to the lattice deformation, and can move only together with it. This makes the effective mass of the localized polaron much higher than the electron mass. The results presented here show, that the same can occur for a proton impurity in the neutron matter. In our calculations the coupling of a proton to the phonons increases with density, and the critical coupling corresponds to critical density for localization of the proton.

An important quantitative difference of the nuclear polaron considered here as compared with the electron one is in the values of the integrals I_2, Eq. (21), and I_1, Eq. (23). They are functions of the ratio $q_{\max}/Q$. It is of the order of 100 in solids while of order 1 in our case and increases with the neutron density. The integral I_2 is thus bigger for the electron in crystals than for the proton in the neutron matter. The phonon contribution in our case is thus of importance at high densities.

In the ground state a single polaron should be at rest, i.e., the center of the probability distribution of the localized proton should not move, minimizing in this way the kinetic energy. Thus at low proton concentrations, when the wave functions of the individual protons do not overlap, we would expect the ground state to be a collection of polarons which have their centers fixed. They could form an arrangement which can become a regular lattice if there is any residual repulsive interaction between protons.

The results found in this paper are based on several model assumptions, whose validity in case of our nuclear polaron problem is less certain than in the case of electrons in crystal. The first one is the use of a Debye approximation when calculating the sum over phonons, Eq. (19). Since the Debye momentum $q_{\max}$ is of the order of the neutron Fermi momentum one can worry that the long-wavelength approximation is not applicable and one should use a momentum-dependent coupling σ. A similar problem occurs in the case of local density approximation which we use in Sec. IV. There also can exist deviations of the proton effective interaction v_{eff} at short distances from the form we use in Eq. (47). In this case also new terms in the Thomas-Fermi energy of neutron matter can be important.

The uncertainties mentioned above are the reason that we restrict ourselves to a simplified treatment of the nuclear polaron problem, and not attempt to solve the problem rigorously. One should regard the results found here as indicative that a proton impurity in neutron matter forms a polaron, whose effective mass can be large at high densities. A detailed microscopic discussion of this problem is presented elsewhere.

This work was supported by KBN Grant No. 2 0204 91 01.

APPENDIX: THE FRIEDMAN-PANDHARIPANDE-RAVENHALL MODEL

The energy density, for uniform matter, in the FPR model is

$$\epsilon=\left[\frac{1}{2m_N}+B_N\right]\tau_N+\left[\frac{1}{2m_P}+B_P\right]\tau_P$$
$$+n^2[a_1+a_2e^{-b_1n}+(\tfrac{1}{2}-x)^2(a_3+a_4e^{-b_1n})]$$
$$+ne^{-b_2n^2}[a_5+a_6n+(a_7+a_8n)(\tfrac{1}{2}-x)^2],$$

where

$$n=n_N+n_P,$$
$$x=n_P/n,$$
$$B_i=(a_9n+a_{10}n_i)e^{-b_3n},\quad i=N,P,$$

and

$$\tau_i=\tfrac{3}{5}(3\pi^2)^{2/3}n_i^{5/3},\quad i=N,P.$$

The parameters are [8] $a_1=1054$ MeV fm^3, $a_2=-1393$ MeV fm^3, $a_3=-2316$ MeV fm^3, $a_4=2859$ MeV fm^3, $a_5=-1.78$ MeV, $a_6=-52$ MeV fm^3, $a_7=5.5$ MeV, $a_8=197$ MeV fm^3, $a_9=89.8$ MeV fm^5, $a_{10}=-59$ MeV fm^5, $b_1=0.284$ fm^3, $b_2=42.25$ fm^6, $b_3=0.457$ fm^3.

The effective mass m_* of the proton impurity in neutron matter is

$$\frac{1}{2m_*}=\frac{1}{2m_P}+a_9n_Ne^{-b_3n_N}.$$

[1] R. B. Wiringa, V. Fiks, and A. Fabrocini, Phys. Rev. C **38**, 1010 (1988).
[2] N. C. Chao, J. W. Clark, and C. H. Yang, Nucl. Phys. **A179**, 320 (1972).
[3] M. Kutschera and W. Wójcik, Phys. Lett. B **223**, 11 (1989).
[4] O. Sjöberg, Nucl. Phys. **A265**, 511 (1976).
[5] G. D. Mahan, *Many-Particle Physics* (Plenum, New York, 1981).
[6] A. S. Davydov, *Solid-State Theory* (in Russian) (Nauka, Moscow, 1976).
[7] T. D. Lee, F. E. Low, and D. Pines, Phys. Rev. **90**, 297 (1953).
[8] J. M. Lattimer, Annu. Rev. Nucl. Part. Sci. **31**, 337 (1981).
[9] B. Friedman and V. R. Pandharipande, Nucl. Phys. **A361**, 502 (1981).
[10] P. Haensel, Nucl. Phys. **A298**, 139 (1978).
[11] J. Nitsch, Z. Phys. **251**, 141 (1972).
[12] M. Kutschera and W. Wójcik, Acta Phys. Pol. B **21**, 823 (1990).
[13] G. Baym, H. A. Bethe, and C. J. Pethick, Nucl. Phys. **A175**, 225 (1971).
[14] J. Bardeen and W. Shockley, Phys. Rev. **80**, 72 (1950).